Personalized Metabolic Assessment of Erythrocytes Using Microfluidic Delivery to an Array of Luminescent Wells

ARTICLE *in* ANALYTICAL CHEMISTRY · APRIL 2009

Impact Factor: 5.64 · DOI: 10.1021/ac900084g · Source: PubMed

5 AUTHORS, INCLUDING:

Nicole V. Tolan
Harvard University
11 PUBLICATIONS **92** CITATIONS
SEE PROFILE

Luiza Iuliana Hernandez
SOMAprobes S.L, San Sebastian, Spain
18 PUBLICATIONS **187** CITATIONS
SEE PROFILE

Wasanthi Subasinghe
University of Kelaniya
9 PUBLICATIONS **165** CITATIONS
SEE PROFILE

Madushi Raththagala
University of Kentucky
12 PUBLICATIONS **101** CITATIONS
SEE PROFILE

Anal. Chem. **2009,** *81,* 3102–3108

Personalized Metabolic Assessment of Erythrocytes Using Microfluidic Delivery to an Array of Luminescent Wells

Nicole V. Tolan, Luiza I. Genes, Wasanthi Subasinghe, Madushi Raththagala, and Dana M. Spence*

Chemistry Department, Michigan State University, East Lansing, Michigan 48824

The metabolic syndrome is often described as a group of risk factors associated with diabetes. These risk factors include, but are not limited to, such conditions as insulin resistance, obesity, high blood pressure, and oxidant stress. Here, we report on a tool that may provide some clarity on the relationship between some of these associated risk factors, especially oxidant stress and hypertension. Specifically, we describe the ability to simultaneously monitor nicotinamide dinucleotide phosphate (NADPH), reduced glutathione (GSH), and shear-induced adenosine triphosphate (ATP) release from erythrocytes using luminescence detection on a microfabricated device. The measurements are performed by delivering erythrocyte lysate (for the NADPH and GSH measurements, two analytes indicative of oxidative stress) or whole red blood cells (RBCs) (for the determination of ATP release from the cells) to an array of wells that contain the necessary reagents to generate a luminescence emission that is proportional to analyte concentration. A fluorescence macrostereomicroscope enables whole-chip imaging of the resultant emission. The concentrations of each NADPH and GSH contained within a 0.7% erythrocyte solution were determined to be 31.06 ± 4.12 and 22.55 ± 2.47 μM, respectively, and the average ATP released from a nonlysed 7% erythrocyte solution was determined to be 0.54 ± 0.04 μM. Collectively, the device represents a precursor to subsequent merging of microfluidics and microtiter-plate technology for high-throughput assessment of metabolite profiles in the diabetic erythrocyte.

The Centers for Disease Control and Prevention reported that, in 2007, diabetes was affecting approximately 23.6 million people in the United States with 17.9 million diagnosed, and more than 5.6 million people unaware of their condition.[1] It was also estimated that another 57 million people in the United States have prediabetes with approximately 25% left undiagnosed. Diabetes is linked to numerous complications such as heart disease and stroke, hypertension, neuropathy, nephropathy, improper circulation leading to amputations in some cases, dental disease, as well as pregnancy complications in women. Efforts to counteract these side-effects include the administration of insulin and various forms of medications to control blood glucose, blood pressure, and lipid content.

In continuance with the complications linked with diabetes, we have recently reported that the ability of the erythrocyte, or red blood cell (RBC), obtained from people with type 2 diabetes to release adenosine triphosphate (ATP) is decreased in comparison to control subjects and that this decrease is associated with oxidant stress in the RBC.[2,3] As a stimulus of nitric oxide (NO) production in the endothelium, RBC-derived ATP has been implicated as a possible determinant in the control of blood flow in vivo. Another report[4] has also shown a decrease in ATP release from the RBCs of people with diabetes that seems to be related to an increase in the glycation of proteins involved in the ATP release pathway. Finally, it has also been shown that RBCs in the absence of metal-activated C-peptide, a substance coreleased with insulin, also release less ATP than those RBCs in the presence of the peptide.[5] Summarily, the various ATP release pathways suggest that multiple factors or metabolic processes may affect ATP release from the erythrocyte, and some of these processes are described in Figure 1.

While studies are still ongoing in our laboratories and others to identify those factors affecting such cellular phenomena as ATP release from RBCs, there are presently no devices available to perform an assessment of metabolic status and cellular function, simultaneously. Such a device would be beneficial because it would not only enable the detection of a possible biomarker for a particular disease (e.g., low ATP release from the RBCs of people with diabetes) but would also be able to provide information toward a therapeutic intervention if the root cause of the decreased ATP release could be determined.

Unfortunately, there are challenges associated with measuring multiple analytes and cell function simultaneously because the measurement of the analytes typically requires cell lysis, whereas cell function would be better studied on the intact cell. A possible approach to solving this problem would be to compartmentalize the required measurements to different areas on a device, thus

* To whom correspondence should be addressed. E-mail: dspence@chemistry.msu.edu. Fax: 517-353-1793. Phone: 517-355-9715, ext 177.

(1) CDC. U.S. Department of Health and Human Services, Atlanta, GA, 2008.
(2) Carroll, J.; Raththagala, M.; Subasinghe, W.; Baguzis, S.; Oblak, T. D.; Root, P.; Spence, D. *Mol. Biosyst.* **2006**, *2*, 305–311.
(3) Subasinghe, W.; Spence, D. M. *Anal. Chim. Acta* **2008**, *618*, 227–233.
(4) Sprague, R. S.; Stephenson, A. H.; Bowles, E. A.; Stumpf, M. S.; Lonigro, A. J. *Diabetes* **2006**, *55*, 3588–3593.
(5) Meyer, J. A.; Froelich, J. M.; Reid, G. E.; Karunarathne, W. K. A.; Spence, D. M. *Diabetologia* **2008**, *51*, 175–182.

10.1021/ac900084g CCC: $40.75
Published on Web 03/20/2009

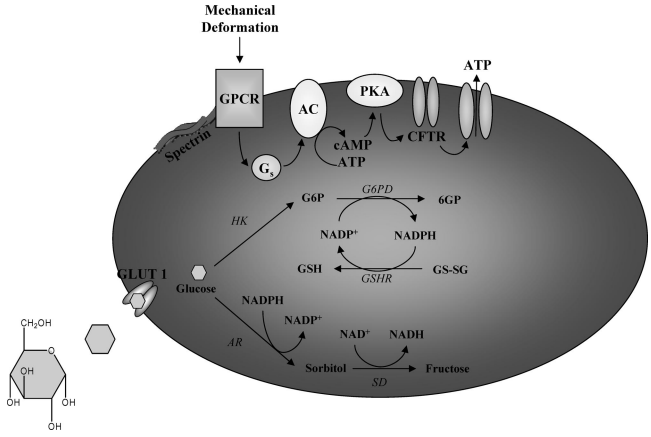

Figure 1. Illustration of the deformation-induced ATP release pathway, highlighting the importance of glucose metabolism via the pentose phosphate pathway. Activation of the G-protein (G_s) coupled receptor (GPCR) by mechanical deformation leads to the conversion of ATP to cyclic adenosine monophosphate (cAMP) by adenylyl cyclase (AC), which results in phosphorylation of the cystic fibrosis transmembrane regulator (CFTR) by protein kinase A (PKA), upon which, stimulates ATP release from the cell. Here, the pentose phosphate pathway includes the conversion of glucose to glucose 6-phosphate (G6P) via hexokinase (HK), leading to the production of NADPH as glucose 6-phosphate dehydrogenase (G6PD) produces 6-phosphogluconolactone (6GP). NADPH is essential in the production of the antioxidant glutathione (GSH) from its disulfide form (GS−SG) by way of glutathione reductase (GSHR). GSH protects spectrin from oxidation and maintains the deformability of the cellular membrane, which is necessary for mechanical deformation-induced ATP release.

facilitating the measurements while at the same time enabling the potential for high-throughput analyses.

Here, we employ a microfluidic device to deliver intact and lysed RBCs through fabricated channels to predetermined microtiter-plate-like wells. The wells are separated from the channels with a porous polycarbonate membrane, similar to our previously reported design.[6,7] These wells are then preloaded with the appropriate reagents necessary for specific (enzymatic-based) reactions that will generate luminescent (fluorescent and chemiluminescent) species. Such a device enables the simultaneous measurement of nicotinamide dinucleotide phosphate (NADPH) and glutathione (GSH), two species that are essential in RBC oxidant defense mechanisms, from lysed RBC fractions. The microfluidic delivery of the samples to the wells is important both analytically and physiologically because the ATP release from the RBCs is stimulated by flow-induced shear stress. By incorporating microfluidic delivery of the intact cells to the wells, a portion of the cellular oxidant status and cellular function can be monitored simultaneously. Moreover, calibration and measurement of the analytes are performed in the presence and absence of various inhibitors on a single device. Furthermore, simultaneous imaging of the wells that are addressed by the underlying channels represent a starting point for attempts to merge microfluidic and microtiter-plate technology.

METHODS

Obtaining Washed Red Blood Cells. RBCs used in this study were obtained from animals following protocols approved by the Animal Investigation Committee at Michigan State University. Male New Zealand white rabbits (2.0−2.5 kg) were anesthetized using ketamine (8 mL/kg, im) and xylazine (1 mg/kg, im) followed by pentobarbital sodium (15 mg/kg, iv). Rabbits were ventilated with room air at a rate of 20 breaths/min using a tidal volume of 20 mL kg^{-1} by placing a cannula in the trachea. A catheter was then placed into the carotid artery for administration of heparin (500 units, iv) prior to exsanguination through the same cathether. Approximately 80 mL of whole blood is collected from each animal. Whole blood was then centrifuged three times at 500*g* at 25 °C for 10 min. After each centrifugation, the plasma and buffy coat were collected for other experimentation before the remaining solution was resuspended and washed twice in a physiological salt solution (PSS) (containing in mM, 4.7 KCl, 2.0 $CaCl_2$, 140.5 NaCl, 12 $MgSO_4$, 21.0 tris(hydroxymethyl)aminomethane, 5.6 glucose with 5% bovine serum albumin at a final pH of 7.4). All samples were prepared and analyzed within 8 h of harvesting from the animal.

Poly(dimethylsiloxane) Array Fabrication. For this application, standard soft lithography techniques, which have been previously described,[8−13] were employed to obtain replica poly(dimethylsiloxane) (PDMS) molds from raised-featured masters. Here, for the individual quantitative determination of NADPH and GSH in RBC samples, a microfluidic device composed of two individual PDMS layers that are irreversibly sealed around a polycarbonate membrane (GE Osmonics, Minnetonka, MN) was fabricated by simply aligning the layers prior to full polymerization in the baking process. Similar methods of thermocuring have been described[11,14−16] in comparison to traditional plasma sealing. As illustrated in Figure 2a, the top layer, which contains 18 wells, houses the fluorescence probe solutions (described below) for both NADPH and GSH, while the bottom layer contains individual channels to deliver RBC-derived analytes to the wells above the membrane. For each device, displacement syringe pumps were used to introduce samples from 500 μL gas tight syringes through Tygon tubing that was fitted with 15 mm, 23 gauge hypodermic steel tubing bent at 90°. This steel tubing was placed in the inlet access holes created in fabrication to deliver solutions directly into the channels.

Each individual layer was obtained by pouring a degassed 5:1 mixture of Sylguard 184 PDMS elastomer and curing agent onto a silicon master with six raised-featured channels (approximately 200 μm wide and 100 μm thick) as well as by pouring a degassed 20:1 PDMS mixture onto a nonpatterned silicon wafer. These PDMS layers were cured individually at 75 °C for 20 min prior to removal from the wafers. Inlet holes and waste reservoirs for each channel were punctured through the channel-patterned PDMS

(6) Genes, L. I.; Tolan, N. V.; Hulvey, M. K.; Martin, R. S.; Spence, D. M. *Lab Chip* **2007**, *7*, 1256–1259.
(7) Tolan, N. V.; Genes, L. I.; Spence, D. M. *JALA* **2008**, *13*, 275–279.
(8) Duffy, D. C.; McDonald, J. C.; Schueller, O. J. A.; Whitesides, G. M. *Anal. Chem.* **1998**, *70*, 4974–4984.
(9) McDonald, J. C.; Duffy, D. C.; Anderson, J. R.; Chiu, D. T.; Wu, H.; Schueller, O. J. A.; Whitesides, G. M. *Electrophoresis* **2000**, *21*, 27–40.
(10) McDonald, J. C.; Whitesides, G. M. *Acc. Chem. Res.* **2002**, *35*, 491–499.
(11) Becker, H. G. C. *Electrophoresis* **2000**, *21*, 12–26.
(12) Dolnik, V. L. S.; Jovanovich, S. *Electrophoresis* **2000**, *21*, 41–54.
(13) Quake, S. R.; Scherer, A. *Science* **2000**, *290*, 1536–1540.
(14) Wu, H.; Huang, B.; Zare, R. N. *Lab Chip* **2005**, *5*, 1393–1398.
(15) Li, M. W.; Huynh, B. H.; Hulvey, M. K.; Lunte, S. M.; Martin, R. S. *Anal. Chem.* **2006**, *78*, 1042–1051.
(16) Unger, M. A.; Chou, H.-P.; Thorsen, T.; Scherer, A.; Quake, S. R. *Science* **2000**, *288*, 113–116.

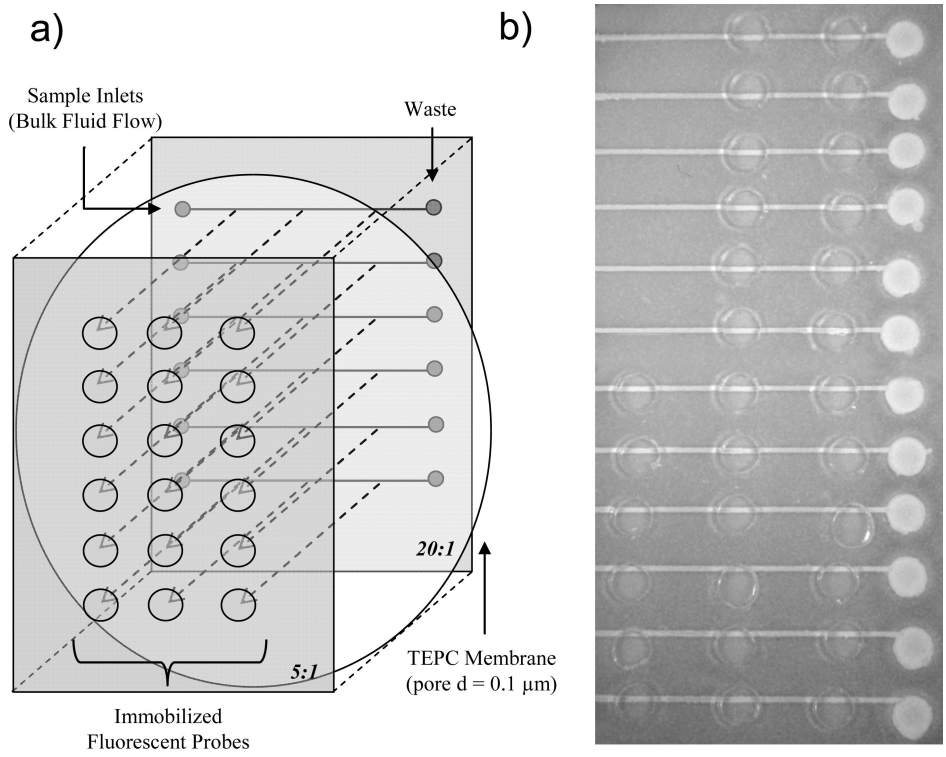

Figure 2. Illustrated in panel a is the schematic drawing of the microfluidic array used for the determination of the metabolites individually. Here, two layers of PDMS, containing parallel microfluidic channels and reactant wells, are sealed around a track-etched polycarbonate (TEPC) membrane with pore diameters of 0.1 μm. The full metabolic profiling for simultaneous determination of NADPH, GSH, and ATP concentrations was performed within the (b) 12-channel 30-well array, which is only slightly altered in the fabrication methods from the original microfluidic array.

layer using a 20 gauge luer stub adapter and a $^1/_8$ in. hole punch, respectively. The wells were constructed by punching 18 holes into the nonpatterned layer using the same $^1/_8$ in. hole punch. The device was completed by aligning the layers and irreversibly curing both chips together around a track-etched polycarbonate membrane (with pore diameters of 0.1 μm) at 75 °C for an additional hour.

This device, shown in Figure 2a, was altered slightly for the fabrication of the microfluidic array used to simultaneously detect all analytes of interest (NADPH, GSH, and ATP). As illustrated in Figure 2b, the microfluidic array was composed of 12 channels containing 30 wells in the top layer, 2 wells for each of the first 6 channels and 3 wells each for the last 6 channels. This allowed for the measurement of NADPH and GSH present in the first six samples (including lysed RBC samples in channels 5 and 6) and for the measurement of ATP released for the last six channels (including nonlysed RBC samples in channels 11 and 12).

Fluorescence determination of NADPH and GSH. Initially, the concentrations of NADPH and GSH were determined within a 0.7% RBC sample on two separate 6-channel, 18-well PDMS microfluidic arrays. For the analysis of NADPH, standard solutions ranging from 12.5 to 200 μM were prepared in phosphate-buffered saline (PBS) solution (containing in g/L, 0.144 KH_2PO_4, 9.00 NaCl, 0.795 Na_2HPO_4 (anhydrous), with a final pH of 7.4 ± 0.1 and mOsm of 287 ± 15) from a 1.0 mM stock solution (8.3 mg dissolved and diluted with PBS to 10 mL). The RBC sample was prepared by diluting the washed RBCs to a 0.7% hematocrit in deionized and distilled water (DDW, 18.1 MΩ resistivity), which resulted in a complete lysis of the cells, thus enabling the intracellular concentrations of the NADPH and GSH to be exposed and subsequently determined.

Standard and RBC sample solutions were pumped at a rate of 1.0 μL/min through the six underlying microfluidic channels for 15 min, allowing the NADPH within each solution to react with the fluorescent probe within the wells above. A volume of 12 μL of a 30 μM resazurin fluorescence probe solution for NADPH, prepared from the Vybrant cytotoxicity assay kit (Invitrogen Corp., Carlsbad, CA), was pipetted into each of the 18 wells within the top layer of the PDMS microfluidic array. When reduced by NADPH, the resazurin fluorescent probe forms red-fluorescent resorufin, with excitation and emission wavelengths of 569 and 587 nm, respectively. Fluorescence images were captured of the entire array using an Olympus MVX fluorescence stereomicroscope (Center Valley, PA), and each well was analyzed for pixel intensities. The MVX was fitted with a resorufin filter cube having λ_{max} excitation and emission wavelengths of 577 and 620 nm, respectively. After a standard calibration curve was constructed from the fluorescence intensities attained from each standard solution, a linear regression analysis (resulting in the line $y = 1.3822x - 47.7190$ and a correlation coefficient of $r^2 = 0.9999$ for the example shown in Figure 3) was used to determine the concentration of NADPH in the lysed RBC sample.

This experiment was repeated using a separate 6-channel, 18-well PDMS array for determining GSH in standards and the same RBC sample. In this instance, the standard solutions ranged from 2.5 to 40 μM and were also prepared in PBS solution from a 1.0 mM stock solution that was prepared by diluting 1 mL of a 10 mM standard solution (0.0307 g in 10 mL of PBS) to 10 mL of

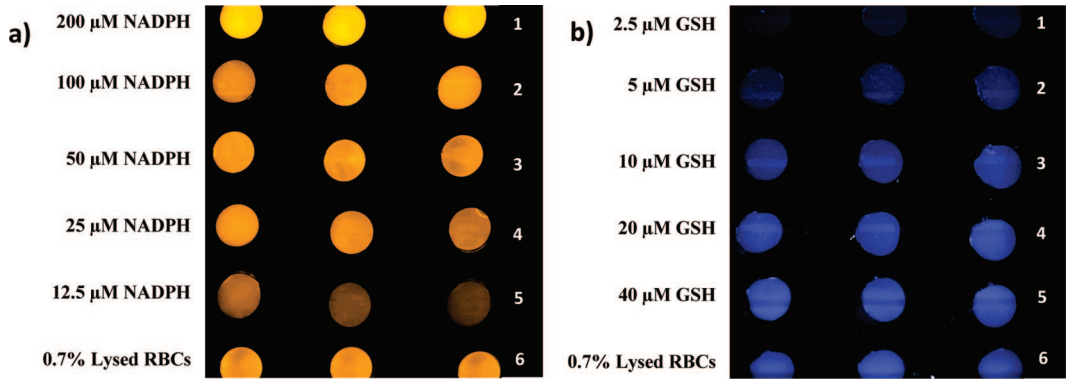

Figure 3. Fluorescence images taken for the initial quantification of (a) NADPH and (b) GSH individually where standard solutions were pumped through channels 1−5 and a single 0.7% lysed RBC sample was pumped through channel 6 for each device. The resulting fluorescent products for NADPH and GSH have emission wavelengths of 587 and 478 nm, respectively.

PBS. Here, the fluorescence probe solution contained monochlorobimane (MCB) and glutathione S-transferase (GST), and again, 12 μL was pipetted into each of the 18 wells prior to pumping solutions through the underlying channels. The MCB solution was prepared to contain 500 μM MCB and 8 U/mL GST, where the GST was added to aid in the binding of GSH to the MCB probe.[2] As above, each solution was allowed to flow through the underlying channels for 15 min and react with the fluorescence probe that had been pipetted into each well. The fluorescence excitation and emission wavelengths for the resulting MCB−GSH product are 370 and 478 nm, respectively. The fluorescence images were captured on the same MVX stereomicroscope fitted with a DAPI fluorescence filter cube with λ_{max} excitation and emission wavelengths of 350 and 460 nm, respectively. The linear regression analysis of the standard solutions (resulting in the line $y = 0.6643x - 5.1557$ and a correlation coefficient of $r^2 = 0.9998$ for the example shown in Figure 3) was used to determine the concentration of GSH present in the lysed 0.7% RBC sample. Initially, the quantitative determination of NADPH and GSH within a 0.7% RBC sample was optimized separately on two individual 6-channel, 18-well arrays, before combining the two assays onto a single device.

Fluorescence Measurements of NADPH and GSH, Simultaneously. By combining both NADPH and GSH into the same standard solutions, each metabolite was effectively measured in the presence of the other and each was quantitatively determined from the same RBC sample. Here, the standard preparation was identical to that described above; however, the incremental standard solutions of NADPH and GSH were prepared in the same volumetric flask. Combining NADPH and GSH in the same standard solutions, while monitoring the fluorescence intensities produced in the two separate columns of wells, allowed for the construction of two separate calibration curves and only required three channels. In the first 6 channels of the 12-channel array, the resazurin probe solution was only loaded in the first column of wells, while the MCB probe solution was loaded into the second column of wells. The isolated and washed RBCs were diluted to a 7% hematocrit in PSS; moreover, one of the samples was incubated in PSS containing 100 μM dehydroepandroesterone (DHEA), a known G6PD inhibitor, for 30 min in order to inhibit glucose-6-phosphate dehydrogenase (G6PD) and purposely lower the GSH and NADPH concentrations in the cell.[17−20] After the 30 min incubation, both cell solutions were diluted to 0.7% and lysed by adding 200 μL of the 7% RBC solutions to 1.8 mL DDW, separately. Again, the concentrations of each metabolite in the two RBC samples were determined using linear regression analysis of the fluorescence intensities for each NADPH and GSH standard concentration.

Chemiluminescence Determination of ATP Release. ATP standards ranging from 0.25 to 1.0 μM ATP were prepared from a 100 μM stock (27.6 mg in 500 mL of DDW) in PSS. In addition, two 7% RBC samples were prepared by diluting the washed RBCs to 7% in PSS; however, one of these RBC samples was incubated in PSS containing 20 μM diamide, a known oxidant for GSH and cell-membrane stiffener.[21,22] The diamide incubation occurred for 15 min prior to starting flow within the array in order to maximize the effect of the diamide solution and because the RBCs are able to recover from the oxidant attack and regain membrane flexibility to near initial levels within 30−40 min.[2] Both RBC samples were pumped though the array for 15 min at which time the images were acquired with the same setup as described above. The excitation lamp was not utilized for the chemiluminescence determination of ATP. Images were obtained with a 5 s exposure time in order to maximize the chemiluminescence imaged. Again, as above, the pixel intensities for the standard solutions were used for linear regression analysis in order to determine the concentration of ATP released from the two nonlysed RBC samples.

RESULTS AND DISCUSSION

It has now been reported that the ATP release from the RBCs of people with type 2 diabetes,[2,4] primary pulmonary hypertension,[23] and cystic fibrosis[24] is significantly less in comparison to

(17) Shantz, L. M.; Talalay, P.; Gordon, G. B. *Proc. Natl. Acad. Sci. U.S.A.* **1989**, *86*, 3852–3856.
(18) Gupte, S. A.; Arshad, M.; Viola, S.; Kaminski, P. M.; Ungvari, Z.; Rabbani, G.; Koller, A.; Wolin, M. S. *Am. J. Physiol.* **2003**, *285*, H2316–H2326.
(19) Leopold, J. A.; Cap, A.; Scribner, A. W.; Stanton, R. C.; Loscalzo, J. *FASEB J.* **2001**, *15*, 1771–1773, DOI:, 1710.1096/fj.1700-0893fje.
(20) Yang, N. C.; Jeng, K. C.; Ho, W. M.; Chou, S. J.; Hu, M. L. *J. Steroid Biochem. Mol. Biol.* **2000**, *75*, 159–166.
(21) Ghigo, D.; Bosia, A.; Pagani, A.; Pescarmona, G. P.; Pagano, G.; Lenti, G. *Ric. Clin. Lab.* **1983**, *13*, 375–381.
(22) Kosower, N. S.; Kosower, E. M.; Wertheim, B.; Correa, W. S. *Biochem. Biophys. Res. Commun.* **1969**, *37*, 593–596.
(23) Sprague, R. S.; Stephenson, A. H.; Ellsworth, M. L.; Keller, C.; Lonigro, A. J. *Exp. Biol. Med.* **2001**, *226*, 434–439.

those RBCs obtained from healthy controls. Figure 1 contains some of the pathways that ultimately may affect ATP release from the RBC, although ATP release measurements alone may not be enough information for proper diagnosis as there are now multiple reports of decreased ATP release in multiple disease states.

Previously, we have shown that ATP release is strongly associated with the concentrations of NADPH and GSH in the RBC.[2,3] In comparison to concentrations found within the RBCs of healthy controls, the concentrations of NADPH and GSH are lower within the RBCs obtained from people with type 2 diabetes.[21,25−30] As an initial step toward an improved screening method, we have chosen to perform quantitative measurements involving nonenzymatic antioxidant status in the RBC. The concentrations of each metabolite, NADPH and GSH, were determined individually on separate devices using aliquots from the same 0.7% lysed RBC sample. NADPH standards ranging from 12.5 to 200 μM and GSH standards ranging from 2.5 to 40 μM were pumped through channels 1−5, while the 0.7% lysed RBC sample was introduced through channel 6 for each array. Resazurin (for NADPH) and MCB (for GSH) fluorescence probes were loaded within each of the wells that comprise the microfluidic array, thus enabling triplicate measurements. The fluorescence images, shown in Figure 3, part a (NADPH) and b (GSH), are a result of the metabolites reacting with the probes above the membrane surface.

When each analyte was optimized on separate microfluidic devices by monitoring the fluorescence intensities of the three wells for each underlying channel, the average was used for the linear regression analysis. This effectively represented the variation associated with the consecutive sample analysis along the channel length and indicated that the reproducibility of each standard fluorescence intensity was appropriate for concentration determination of the analytes within the RBC samples. The linear velocity of 1.0 μL/min was chosen along with the internal pore diameter of 0.1 μm to minimize the bulk fluid flow through the polycarbonate membrane, preventing dilution of the fluorescence probe solution located in the wells.

For each sample analysis, background subtraction was performed and standard solutions were incorporated onto each device in order to reproducibly and accurately determine analyte concentrations with the RBC samples. The experimentation was performed intentionally to allow for only a single dependent variable, the analyte concentrations, eliminating any inconsistencies within the setup including, but not limited to, variable excitation and emission intensities resulting from the wavelength selection filter cubes, any possible cross-talk between wavelengths, and heterogeneity of channel−well interface surface area. Here, standard and sample solutions were analyzed approximately 30 min after preparation in order to keep analyte degradation within solution minimal and consistent. More specifically, each solution was pumped through the underlying channels in a manner that would take into account the reaction kinetics between the analytes and the fluorescent probe solutions and the incubation time was determined by the commencement of fluid flow.

RBC samples were also incubated with various reagents to provide validation of the NADPH and GSH measurements. For example, some RBCs were incubated with 100 μM DHEA prior to measuring the NADPH and GSH. Similarly, the concentration of ATP release was determined from RBCs incubated with and without 20 μM diamide, a substance known to reduce GSH concentrations and stiffen cell membranes. Figure 4 contains the experimental setup and contains the images used to determine the overall antioxidant status of the cell and the resulting ATP release. Here, 12 μL of the fluorescence probes, resazurin (labeled as RES) and monochlorobimane with GST (labeled as MCB), was pipetted into individual wells that comprised the two columns for channels 1−6 to determine the concentration of NADPH and GSH. In a similar manner, 12 μL of the luciferin and luciferase solution (labeled as L/L) was pipetted in the wells that comprise all three columns, illustrating the ability to integrate triplicate measurements, for channels 7−12 to determine shear-induced ATP release. Standard solutions of NADPH and GSH ranging from 25 to 200 μM and 5 to 40 μM, respectively, were combined and pumped through channels 1−4, where the metabolites in solution react with their corresponding fluorescence probe in each well. Standard ATP solutions ranging from 0.25 to 1.0 μM were pumped through channels 7−10, where the chemiluminescence produced in the absence of the fluorescence excitation source is imaged simultaneously. As before, intensities of each well were measured and used to construct a calibration curve for the quantitative analysis of NADPH, GSH, and ATP within each sample.

As shown in Figure 5a, the 0.7% RBC sample was determined to contain on average 31.06 ± 4.12 μM NADPH and 22.55 ± 2.47 μM GSH, which, upon G6PD inhibition using DHEA, was reduced to 22.99 ± 4.63 μM NADPH and 14.60 ± 3.14 μM GSH, where the variance is reported as the standard error of the mean. Figure 5b illustrates the results for the quantitative determination of ATP release and is given as average micromolar amounts where the variance is expressed as standard error of the mean. The concentrations of NADPH and GSH for the 0.7% lysed RBC sample without DHEA incubation are 377 ± 50 and 274 ± 30 amol/RBC, respectively, falling within the range reported elsewhere using various methods.[25,26,28,30−32] Here, the concentration of ATP released from a 7% RBC sample was determined to be 0.54 ± 0.04 μM which was reduced to 0.34 ± 0.04 μM when incubated with diamide prior to analysis. ATP release, indicative of the shear forces that are exerted on the RBCs, is specific to the channel dimensions of this particular microfluidic device as well as the linear rate of the samples through the underlying channels. Here, the linear rate for this device is approximately 3-fold greater than that found within 50 μm i.d. microbore tubing, indicating ATP release that is notably equivalent to 0.190 ± 0.01 μM, as previously reported.[2]

(24) Sprague, R. S.; Ellsworth, M. L.; Stephenson, A. H.; Kleinhenz, M. E.; Lonigro, A. J. *Am. J. Physiol.: Heart Circ. Physiol.* **1998**, *275*, H1726–1732.
(25) Costagliola, C. *Clin. Physiol. Biochem.* **1990**, *8*, 204–210.
(26) Aaseth, J.; Stoa-Birketvedt, G. *J. Trace Elem. Exp. Med.* **2000**, *13*, 105–111.
(27) Beard, K. M.; Shangari, N.; Wu, B.; O'Brien, P. J. *Mol. Cell. Biochem.* **2003**, *252*, 331–338.
(28) Dincer, Y.; Akcay, T.; Alademir, Z.; Ilkova, H. *Metab., Clin. Exp.* **2002**, *51*, 1360–1362.
(29) Bravi, M. C.; Pietrangeli, P.; Laurenti, O.; Basili, S.; Cassone-Faldetta, M.; Ferri, C.; De Mattia, G. *Metabolism* **1997**, *46*, 1194–1198.
(30) De Mattia, G.; Bravi, M. C.; Laurenti, O.; Cassone-Faldetta, M.; Armiento, A.; Ferri, C.; Balsano, F. *Metabolism* **1998**, *47*, 993–997.
(31) Raththagala, M.; Root, P. D.; Spence, D. M. *Anal. Chem.* **2006**, *78*, 8556–8560.
(32) Cereser, C.; Guichard, J.; Drai, J.; Bannier, E.; Garcia, I.; Boget, S.; Parvaz, P.; Revol, A. *J. Chromatogr., B: Biomed. Sci. Appl.* **2001**, *752*, 123–132.

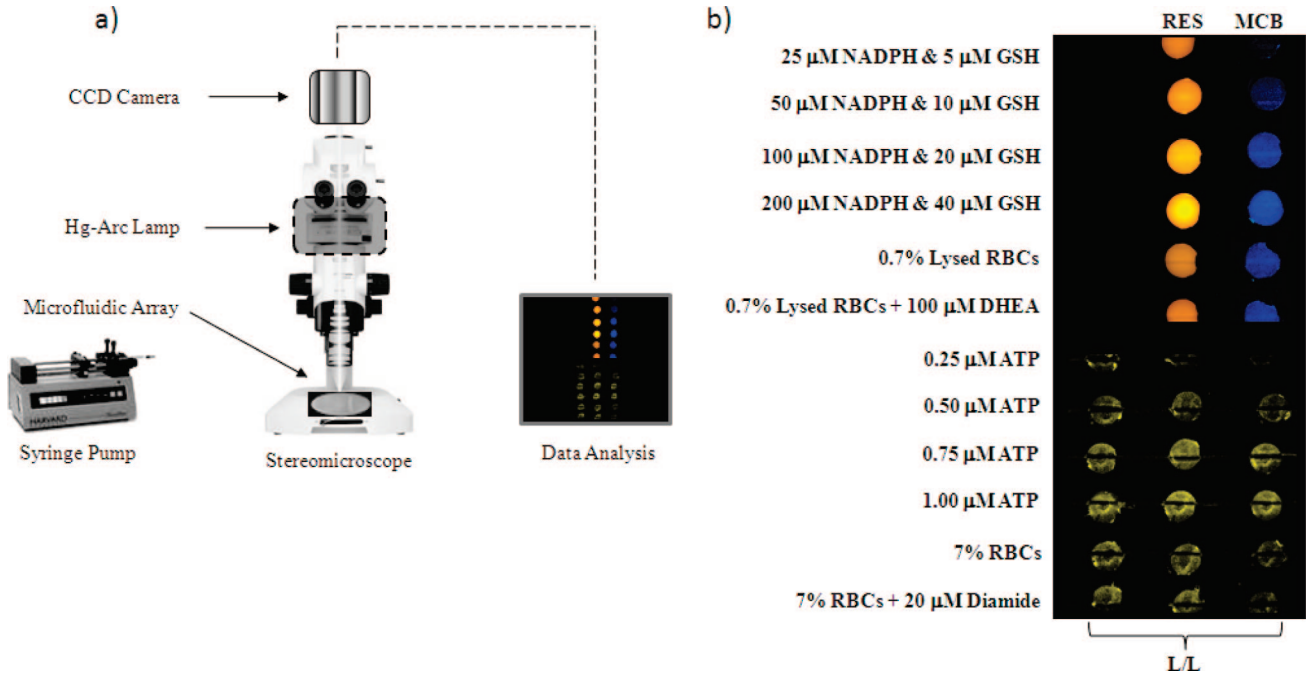

Figure 4. Illustration of the (a) microscopy setup used to obtain fluorescent and chemiluminescence images for the (b) metabolic profiling to determine the concentrations of NADPH and GSH found within, as well as ATP released from, various RBC sample solutions. Standard solutions containing both NADPH and GSH were allowed to flow through channels 1−4, while standard samples of ATP were pumped through channels 7−10 which were used to determine the concentrations of each analyte in 0.7% RBCs, 0.7% RBCs plus DHEA, 7% RBCs, and 7% RBCs plus diamide. Here, 12 μL of the fluorescence probes, resorufin (RES) and monochlorobimane (MCB), was contained in individual columns of wells (channels 1−6) for the determination of NADPH and GSH concentrations, whereas 12 μL of a luciferin and luciferase solution (L/L) was localized in the wells for each column of wells (channels 7−12) for the determination of shear-induced ATP release. The standards and samples were pumped through the underlying microfluidic channels at a rate of 1.0 μL/min for 15 min allowing the analytes of interest to react with the probes contained in each individual well. Pixel intensities, corresponding to the fluorescence intensities of each well, were measured and used to construct a calibration curve for each column of the device. The concentrations of each analyte were then determined using the resulting least-squares regression analysis and reported as micromolar concentrations with variances corresponding to the standard error of the mean.

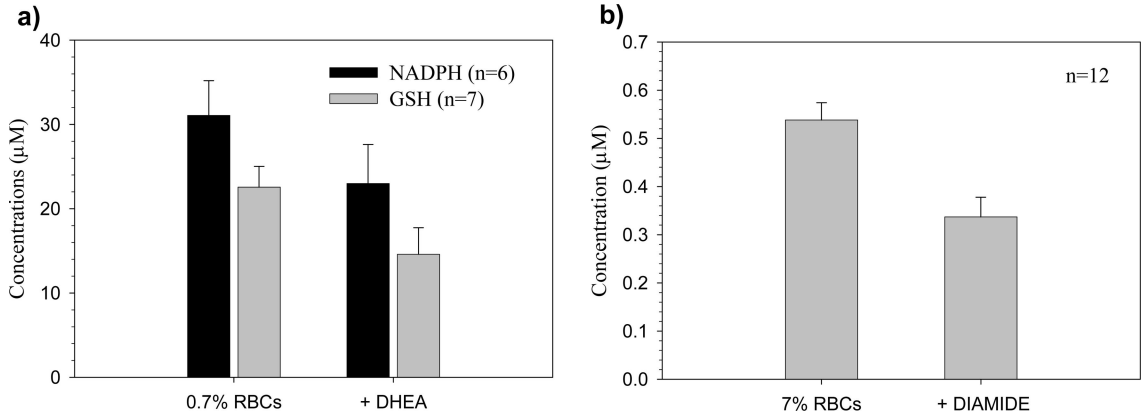

Figure 5. Concentrations of (a) NADPH, GSH, and (b) ATP determined for lysed and nonlysed RBC samples. Specifically, the concentrations of NADPH and GSH for 0.7% RBC samples were determined to be 31.06 ± 4.12 and 22.5 ± 2.47 μM, respectively; the concentrations decreased for each upon the incubation of DHEA to 22.9 ± 4.63 and 14.6 ± 3.1 μM, respectively. The concentration of ATP release within the flow-based microfluidic array fabricated here was determined to be 0.54 ± 0.04 μM for a 7% RBC sample which was reduced to 0.34 ± 0.04 μM when incubated with diamide. Error bars represent the SEM for the number of rabbits indicated in the figures.

CONCLUSIONS

The ability to determine the concentrations of NADPH, GSH, and ATP from RBC samples treated to reflect the state of RBCs obtained from diabetic patients is demonstrated here. It is anticipated that this methodology will allow for the differentiation of RBCs obtained from diabetic patients, compared to those obtained from healthy nondiabetic controls. This microfluidic array allows for multiple optical detection methods (fluorescence and chemiluminescence) to be used simultaneously, while also incorporating a flow-based system without the need for sample preparation due to the separation of the wells from the channels by a polycarbonate membrane. Expansion to nonoptical modes of detection, such as amperometric, is possible based on recent reports of integrated electrodes in microfluidic devices. Here, simultaneous analysis performed on a single platform may serve

as diagnostic tool for determining the cause for hypertension complications as it relates to diabetes.[33] This study illustrates the ability to profile various analytes from within a lysed RBC solution, as well as analytes released from intact RBCs.

Monitoring the concentrations of NADPH, GSH, and ATP on a single device is an initial attempt at merging metabolic profiling with cell function assays simultaneously. Because different diseases often have common metabolic traits, we feel that the device described here may improve molecular diagnostics. For example, people with cystic fibrosis have RBCs that release very little ATP due to a reduced activity of the cystic fibrosis transmembrane regulator protein (CFTR).[24] However, as mentioned above, people with diabetes have similar ATP release patterns. Collectively, if a blood (or RBC) sample was to be screened for ATP release and the release was found to be lower than normal, it would be premature to conclude the subject has cystic fibrosis unless more quantitative information about the sample was obtained. A glycated hemoglobin value, which is generally higher in the poorly controlled diabetic but often normal in people with cystic fibrosis, could be obtained to learn more about the initial screen. Therefore, coupling a quantitative determination of ATP with another measured parameter would be useful, if not necessary.

Accordingly, the device and methodology described here also serves as the foundation for the application to individualized drug efficacy and ADMET (absorption, distribution, metabolism, excretion, toxicity) studies by integrating the very relevant aspect of blood flow. Recently, the cost of pharmaceutical testing for a drug candidate has risen to 400 million dollars on average, increasing the overall cost of bringing a new drug to the market to 1.2 billion dollars.[34] The ability to more effectively test drug candidates within a better mimic of the in vivo system by incorporating flow and multiple cell types would not only reduce the number of candidates that reach the clinical trial phase only to fail but, also, would indicate the effectiveness many drugs may possess and are only evident within a flow-based system. An example here is pentoxyfilline, which is known to improve blood flow in vivo. Our group[35] has reported that pentoxyfilline results in the release of RBC-derived ATP, but only in the presence of flow-induced shear. In contrast, under static conditions, pentoxyfilline has no effect on the RBCs. Thus, it is anticipated that the device described here may improve ADMET studies by incorporating blood components, flow, and, possibly, multiple cell types in a device that may be amenable to high-throughput plate readers.

ACKNOWLEDGMENT

This work was funded by the National Institutes of Health (NIDDK R01 DK071888-01A2) and Michigan State University.

Received for review January 13, 2009. Accepted February 20, 2009.

AC900084G

(33) Hood, L.; Perlmutter, R. M. *Nat. Biotechnol.* **2004**, *22*, 1215–1217.

(34) Malakoff, D. *Science* **2008**, *322*, 210–213.

(35) Carroll, J. S.; Ku, C.-J.; Karunarathne, W.; Spence, D. M. *Anal. Chem.* **2007**, *79*, 5133–5138.